Published in final edited form as:
Soft Matter. 2014 March 14; 10(10): 1439–1449. doi:10.1039/c3sm50854d.

Polyelectrolyte properties of filamentous biopolymers and their consequences in biological fluids

Paul A. Janmey[1], **David R. Slochower**[1], **Yu-Hsiu Wang**[1], **Qi Wen**[2], and **Andrejs Cebers**[3]

[1]Institute for Medicine and Engineering, University of Pennsylvania, 1010 Vagelos Laboratories, 3340 Smith Walk, Philadelphia, PA 19104 USA

[2]Dept. of Physics, Worcester Polytechnic Institute, 100 Institute Road, Worcester, MA 01609-2280 USA

[3]Laboratory of Soft Materials, Department of Theoretical Physics, University of Latvia, Zellu 8, LV-1002, Latvia

Anionic polyelectrolyte filaments are common in biological cells. DNA, RNA, the cytoskeletal filaments F-actin, microtubules, and intermediate filaments, and polysaccharides such as hyaluronan that form the pericellular matrix all have large net negative charge densities distributed over their surfaces. Several filamentous viruses with diameters and stiffnesses similar to those of cytoskeletal polymers also have similar negative charge densities. Extracellular protein filaments such collagen, fibrin and elastin, in contrast, have notably smaller charge densities and do not behave as highly charged polyelectrolytes in solution. This review summarizes data that demonstrate generic counterion-mediated effects on four structurally unrelated biopolymers of similar charge density: F-actin, vimentin, Pf1 virus, and hyaluronan, and explores the possible biological and pathophysiological consequences of the polyelectrolyte properties of biological filaments.

Introduction

Targeting of proteins such as DNA polymerases, actin crosslinking proteins and molecular motors to their filamentous ligands often involves positively charged protein domains that stabilize interactions both by direct electrostatic binding to the polyelectrolyte but also by the entropy gained when smaller valence counterions such as K+ or Na+ are displaced by the multicationic ligand. Long rigid or semi-flexible polymers with fixed charges spaced closer than the Bjerrum length, the characteristic length below which electrostatic interactions are stronger than thermal energy, acquire fascinating and in some cases counterintuitive properties compared to smaller soluble charged solutes. The Bjerrum length is defined as

$$\lambda_B = \frac{e^2}{4\pi\varepsilon_0\varepsilon_r k_B T},$$

where *e* is the elementary charge, ϵ_r is the relative dielectric constant of the medium and ϵ_0 is the vacuum permittivity. For water at physiologically relevant temperature $\lambda_B \approx 0.7$ nm, and the spacing between fixed charges in many biopolymers is less than that distance.

The pioneering work of Manning and others showed that the effective electrostatic charge of a biopolymer, as judged for example by its electrophoretic mobility, is not equal to its bare charge density, but to a lower value with charges spaced so that the distance between them does not exceed a linear density equal to the inverse Bjerrum length [1, 2]. The factor by which the net charge on the polyelectrolyte is reduced depends on the valence Z of the counterion, according to the expression:

$$\begin{array}{ll} r=1-(Z\zeta)^{-1} & \text{for } Z\zeta>1 \\ r=0 & \text{for } Z\zeta<1, \end{array}$$

where $\zeta = e^2\epsilon_0\epsilon_r k_B T b = \lambda_B/b$ and *b* is the linear charge spacing of the polyelectrolyte in the absence of any associated ions. If the counterions have a mixture of valences, then they will compete for binding to the polyelectrolyte and there is not a general expression to determine the amount by which the net charge on the polyelectrolyte is reduced.

The precise nature of the forces that distribute counterions and co-ions in the vicinity of the charged polymer have been the subjects of many theoretical studies [3–7]. An essential feature of the localized or condensed counterions is that although they are restricted from diffusion away from the long axis of the polymer, they are mobile within a thin volume along its surface. An effect that is vital to the biological relevance of counterion condensation is that univalent counterions can be displaced by a smaller number of divalent or multivalent counterions to maintain approximately the same effective surface charge density. As a result, the free energy change when multivalent cations or polycationic protein domains localize to anionic filaments is dominated by the gain of entropy as a larger number of univalent cations are displaced, and therefore this binding is not screened out at physiologically relevant salt concentrations.

Among the intriguing properties of rodlike polyelectrolytes in aqueous solutions, which have attracted much theoretical and experimental attention, reviewed in [8], are strong attractive interactions between like-charge filaments mediated by multivalent counterions. Such counterion mediated attractions can result in network formation [9–13], or more commonly in collapse of the polyelectrolyte into bundles [14–17], toroids [18], rings [19–21], or other, often lamellar aggregates [22, 23] depending on predictable features of the system such as polymer and counterion concentration, polymer length and stiffness, and the surface distribution of fixed charge on the polyelectrolyte [24–26]. The generic nature of counterion-mediated effects on polyelectrolytes is often neglected in studies of biological systems [27], but the effect is important in pathological cases where intracellular polyelectrolytes enter the extracellular space, such as the thickening of mucus by DNA during cystic fibrosis or the inactivation of antimicrobial peptides by cytoskeletal polymers or bacterially expressed polyelectrolytes.

Polyelectrolytes in the cytoplasm and nucleus

The cytoplasm of most cells is permeated by a three-dimensional network formed of filamentous cytoskeletal polymers, and the nucleus is crowded with DNA and other nucleic acid polymers. Cytoskeletal networks composed of three different polymer types, F-actin, microtubules (MTs) and intermediate filaments (IFs) are generally considered the structures that provide mechanical strength to the cell interior, and have been a model system for the study of crosslinked semi-flexible polymer networks [28, 29]. They also have surface charge densities similar to that of double stranded DNA [28, 30] and provide a surface area greater than that of cellular lipid bilayers on which proteins can dock and enzymatic reactions may be enhanced [31]. DNA and RNA, aside from their essential functions in encoding genetic information, are increasingly recognized as organizers of nuclear mechanics and spatial segregation [27].

The number of ligands for the cytoskeleton, especially the actin filament system, as well as for DNA and RNA, is bewilderingly large. While there are only a handful of well-characterized monomeric (G)-actin binding proteins, there are over a hundred reported ligands for F-actin [32]. These proteins generally lack an obvious sequence homology to explain their common mode of interaction with the limited, uniquely-defined exposed surface of the actin subunits in the filament, but their actin binding sites are generally cationic. For example, the abundant actin-binding protein tropomyosin is a 41 nm long almost completely coiled-coil protein without an obvious unique actin binding site and no affinity for G-actin, but with highly selective and regulated binding to F-actin. The tropomyosin dimer has a large net negative charge, but also a significant number of cationic amino acids [33]. It, like F-actin and other polyelectrolytes, undergoes a sharp transition from isotropic solution to filamentous paracrystals when a critical concentration of divalent cations is added [34]. A specific, localized, binding site for the muscle regulatory protein troponin was identified on tropomyosin decades ago, but similar binding site for F-actin remains undiscovered [35]. Rather than a single actin binding site, tropomyosin has been inferred to have on the order of 14 F-actin binding sites based on sequence homology repeats and evolutionary preservation, and these sites are characterized by having positive charges [35]. Modeling of the tropomyosin coiled-coil shows what although the net charge of the dimer is negative, most of the numerous positively charged sides of the polypeptide are arranged on one face of the helix and that tropomyosin docks in an electrostatic minimum within the groove of the actin filament [36, 37]. The thin filament of the sarcomere and cytoskeletal actin filaments lined by tropomyosin would therefore have an even greater negative charge density than bare F-actin.

There is also increasing evidence that the same protein can bind to two or more different types of cytoskeletal filaments. The microtubule associated proteins MAP2 and tau are perhaps the best known such proteins, as they bind both F-actin and microtubules in vivo [38] as well as in vitro [39]. The binding site to both these filaments appears to be a small cationic region in both tau and MAP2c. Synapsin I also binds both F-actin and microtubules [40, 41] as do the MT binding proteins CLASP 1 and 2 [42]. Calponin binds F-actin and intermediate filaments [42, 43], and the protein plectin is well characterized to bind all three cytoskeletal

filaments [44, 45], with the same domain used to bind both F-actin and vimentin [46]. Several glycolytic proteins also bind more than one cytoskeletal filament type [47, 48].

Cytoskeletal polymers are also strong ligands for a variety of metal ions, polyamines, and cationic peptides, and the binding of these species can produce a variety of specific structures. Indeed polylysine, spermine, lanthanide ions, and histones are among the most potent actin bundling agents identified [49], and it is notable that these polycations are also strong condensing agents for DNA [50].

In contrast to the abundance of semiflexible linear polyelectrolytes within the cell, they are rarely found under normal conditions in the extracellular space. Both eukaryotic and prokaryotic cells often express large anionic polysaccharides or sulfated proteoglycans that remain associated with the cell membrane to form a glycocalyx, the mucus lining most epithelial surfaces is composed of polyanions, and specialized compartments such as joint fluid and the interior of the eye are enriched in anionic polymers such as hyaluronic acid, but these polymers are highly flexible with persistence lengths of a few nanometers, as opposed to the much larger persistence lengths of DNA and especially the cytoskeletal filaments. The more rigid extracellular matrix polymers such as collagen, fibrin and elastin, which constitute the bulk of the extracellular matrix have very low surface charges, with spacing between fixed charges greater than the Bjerrum length, the quantity normally used to define strong polyelectrolytes. It is also notable that the net charges of both collagen 1 triple helices, and the elastin monomer, are positive rather than negative, although the surface charges of the native fibers formed by these proteins are likely to be near neutral or slightly negative due to binding of acidic proteoglycans to their surface [51]. A summary of the area charge densities of several biopolymers is shown in Figure 1.

All cytoskeletal polymers: actin, tubulin, and intermediate filament proteins, are strong polyelectrolytes. Depending slightly on the species, isoform, and type of tightly bound nucleotide, actin monomers carry a nominal charge of −13, tubulin dimers a charge of −53, and a representative intermediate filament protein like vimentin, a charge of −19. These features do not alone provide any special electrostatic properties, but what makes cytoskeletal proteins different from other cytoplasmic elements is their assembly into linear polymers, and these negatively charged filaments have electrostatic properties fundamentally different from those of individual subunits as recognized decades ago by Oosawa [52]. The difference arises not because polymerization alters the net charge per subunit, but because pulling together separate charged subunits into a polymer places the negative charges nearer each other than they would be if each subunit were randomly dispersed, and the resulting electric field from a charged line decays more gradually with distance than does the field from a single protein modeled as a charged point. Two other biological polymers that have charge densities similar to those of cytoskeletal polymers are the filamentous virus Pf1, which has a length of 2 microns, and a diameter and charge density that are very similar to those of F-actin [53, 54] and hyaluronan (HA), the long semi-flexible anionic polysaccharide that forms the pericellular matrix as the well as the transparent gel in the vitreous body of the eye [55], which differs from the other biopolymers considered here by its much smaller persistence length (4 to 8 nm).

Figure 1 shows the molecular structures of segments of DNA, F-actin, vimentin filaments, and Pf1, with their anionic and cationic charge densities highlighted in color. Whereas these four polymers have approximately comparable surface charge densities, the spatial distributions of charges on their surfaces are different, and their highly variable persistence lengths imply that their configurations in aqueous solution will also be different.

The surface charge densities shown in figure 1 are approximations because they depend on the effective diameter of the filaments, which in the case of F-actin is inexact since the cross section of an actin filament is not circular. The effective surface charges are also likely to be underestimates for vimentin because they do not take into account multiple potential phosphorylation sites that would add to its anionic charge. However, the magnitude of these uncertainties is small compared to the difference in surface charge of extracellular filaments like fibrin, which is an order of magnitude smaller. The two other extracellular polymers, collagen and elastin both carry net positive charges on the polymer backbone and become either neutral or possibly slightly anionic only if they bind polyanionic ligands. These examples emphasize the systematic charge differences between intracellular and extracellular polymers.

The polyelectrolyte effects of naturally biopolymers, especially the cytoskeletal filaments are, of course, only one of the factors that govern their interactions with each other and with their many ligands. The surface distribution of negative charges is generally not uniform, with charge clusters space at nm scale intervals and with numerous positive charges displayed on the surface of the net negatively charged polymers. Intermediate filaments (IF) in particular have complex charge distribution, and strong attractions between alternative positive and negative charge domain are an important feature of the self-assembly of IFs from their constituent subunits [56, 57] and similar electrostatic attractions in addition to other more specific binding sites can form crosslinks between IFs. Neurofilaments for example, have complex charge patterns on long unstructured sidearms that protrude from the filament core [58], and charge-dependent interactions among these sidearms also contribute to filament crosslinking [59–61]. Nevertheless, addition of divalent cations to vimentin, neurofilaments, and other IF networks strongly enhances their gelation and increases their elastic moduli to much higher levels than are observed in solutions containing only monovalent counterions [62, 63].

Bundling of structurally diverse polyelectrolytes by multivalent counterions

The similar average charge densities of structurally unrelated polymers seen in Figure 1 contrasts with larger differences in the detailed pattern of charges displayed on the surfaces of these for model polymers. When averaged over scales on the order of 10 nm^2, roughly the size of a filament subunit, the charge densities of several biopolymers are similar, but on a scale less than 1 nm^2, the charge distributions are in some cases (e.g. F-actin and microtubules) highly non-uniform. These local scale charge heterogeneities likely lead to quantitative differences between the electrostatic properties of different filaments, but it is remarkable that the larger scale similarities lead to similar reactions of structurally distinct filaments in solutions with multivalent counterions as shown in Figure 2.

The concentration of counterions at which 5 different types of polyelectrolyte filaments form bundles, as judged by abrupt increases in light scattering depend strongly on the valence of the counterion, but are similar for different polyelectrolytes, and similar when structurally different counterions of similar net cationic charge are compared. For example, greater than 10 mM concentrations of Ca^{2+} and Mg^{2+} are sufficient to bundle F-actin, vimentin and Pf1 virus, and Mn^{2+} can form bundles with these polymers at slightly lower concentrations below 10 mM. The stronger bundling activity of Mn^{2+} has previously been noted for DNA, which is not bundled by Ca^{2+} or Mg^{2+} in aqueous solution unless a co-solvent is added to reduce the dielectric constant, but 50 mM Mn^{2+} is capable of bundling double stranded DNA [64]. The trivalent cation cobalt hexamine bundles F-actin, DNA, and the filamentous fd virus, a structurally similar but shorter analog of Pf1 at very similar concentrations of a few mM. Two structurally unrelated tetravalent cations spermine and the antimicrobial agent CSA13 bundle both F-actin and DNA at sub mM concentrations, and the larger higher valence counterions LL37, lysozyme, and a 16-mer of lysine bundle these polymers as well as fd virus at μM concentrations. The critical cation concentrations needed for bundling denoted in Figure 2 have mainly been measured in solutions with ionic strength contributed by monovalent counterions less than that of most biological fluids. However, when the effects of monovalent ions have been systematically studied, they compete only weakly with multivalent counterion, and inclusion of physiologically relevant (150 mM) concentrations of Na^{+} or K^{+} increases the critical bundling concentration only less than an order of magnitude [30, 65–68].

Network and lamellar phases formed by polyelectrolytes and counterions

Counterion-induced condensation of polyelectrolyte filaments into bundles and toroids has been the best experimentally characterized transition of these systems in part because the transition is sharp and leads to changes in light scattering, birefringence, sedimentation, and other properties that can be precisely quantified and to structures that can be resolved by light and electron microscopy. However, theoretical studies suggest that numerous other morphologies of semiflexible or rigid polymers mediated by multivalent counterions can form at counterion concentrations lower than those required for collapse into bundles, if the biopolymers are sufficiently long and the samples can be prepared with minimal shearing [25, 26]. Scattering and imaging techniques have revealed fascinating structures, often lamellar or tubular, arising from the interaction of DNA [69, 70], F-actin [13, 71], microtubules [15], and neurofilaments [72] with multivalent counterions, especially cationic lipids. X-ray scattering studies have been especially effective in discriminating nm scale structures within polyelectrolyte systems that have been aggregated by multivalent counterions. For example, X-ray scattering has revealed dynamic clusters of counterions near patches of F-actin that are enriched in negative charge [73], and studies of neurofilaments have revealed fascinating liquid crystalline structures formed by the polypeptides that extend from the filament surface and make contact with each other [59, 74]. Some of these structures were not predicted by theory, and a range of structures formed by polyelectrolyte systems have been summarized in recent reviews [8, 72].

Not only can multivalent cations reorganize the structure of cytoskeletal polymers and other polyelectrolytes, but these polymers might act also act as buffers for selected counterions in

the cytoplasm. The concentration of negative surface charges on the cytoskeleton is on the order of several mM, and therefore sufficient to buffer the bulk of ions such as Ca^{2+}, Mg^{2+}, Zn^{2+} or spermine^{4+}, which are the most abundant multivalent cations in the cell. Indeed a role for the cytoskeleton has been prosed as both a buffer and conduit for Ca^{2+} fluxes that arise as channels open in the plasma membrane between intracellular and extracellular compartments with resting free Ca^{2+} concentration in the range of 100 nM to 2 mM, respectively [75, 76].

A particularly interesting and relatively underexplored counterion-dependent structure of filaments is the lattice or crosslinked network phase, predicted to form when the polyelectrolytes are very long but dilute enough to be below the isotropic-nematic transition, and the counterion concentration is less than that at which bundle formation occurs, which may correspond to conditions in the cell. Figure 3A shows the structure of a crosslinked raft network formed by F-actin and divalent metal ions inferred from X ray scattering data [13] from initially isotropic F-actin systems to which divalent cations were added to concentrations below those shown in Fig 2 to induce bundling. More recently, complex networks composed of single actin filaments and filament bundles have been directly visualized by slowly concentrating both F-actin and Mg^{2+} by evaporation from drops (Figure 3B) or by infusion of Mg^{2+} into F-actin in a microfluidic device (Figure 3C). These images show complex ordered structures characterized by linking of multiple filament bundles into nodes, and higher resolution images also show meshworks and ladder-like structures containing thinner fibers and presumably single filaments. The network and node spacing and other geometrical factors in these systems depend on the length scale and shape of the confined volumes in which these networks form, but the assembly is clearly dependent on the presence of sufficient concentrations of multivalent counterions.

Structures such as those shown in Figure 3 suggest that interconnected systems of polyelectrolytes stabilized by counterions will have rheological properties with some similarity to those of crosslinked polymer gels. Direct effects of divalent metal ions or multivalent cations on the rheology of filamentous polyelectrolytes are beginning to be revealed, but in many cases it is difficult to separate the generic and polyelectrolyte-dependent contribution to rheological changes from the effects of specific binding of metal ions to proteins or nucleic acids. Evidence that non-specific electrostatic interactions can lead to gelation of F-actin was seen in a study in which a large polycationic tertiary amine-derivatized acrylamide polymer solution was slowly diffused into a solution of actin. After the polycation diffused into the volume containing F-actin, even very low concentrations (0.01 mg/ml) of F-actin could form gels with Young's moduli of 1 Pa[11]. By comparison, the linear Young's modulus of 0.3 mg/ml F-actin crosslinked by the actin-binding protein scruin ranges from 0.5 to 2 Pa, depending on crosslinking density (Fig. 2C from [77]). Intermediate filaments, in particular neurofilament suspensions, have been clearly shown to increase viscosity with increasing Mg^{2+}, and to form viscoelastic gels at $[Mg^{2+}] > 5$ mM [78, 79]. Vimentin filaments also form gels with elastic moduli that depend on the concentration of divalent cations [63], especially Mg^{2+} as seen in Figure 4.

Effects of divalent cations on rheology of cytoskeletal polymer networks have generally been attributed to the binding of these ions to specific sites on the natively folded surface of

the proteins within the polymers rather than to the same type of generic counterion-dependent effects that govern the bundling transition. There is evidence for preferential binding of divalent cations to sites formed at the junctions between actin subunits in a filament [80] that can promote actin polymerization, and for structures protruding from the surface of neurofilaments [60] or vimentin [63] that might bind preferentially to divalent cations and therefore act as a specific crosslinker between filaments. However, the generic effect of counterion condensation on the filaments is difficult to differentiate, especially when the concentration of divalent cations required to increase the elastic moduli of cytoskeletal networks is orders of magnitude greater than the critical crosslink density needed for gelation, and close to that where structures like raft phases and other crosslinked structures are predicted from theory.

More direct evidence for gelation of polyelectrolytes by multivalent counterions is provided from studies of the rheology of the filamentous virus Pf1. This bacteriophage is structurally similar to fd virus, which has been extensively used to characterize nematic and other liquid crystalline phases [81]. However, fd is so short (800 nm) that it forms nematic phases at concentrations near that at which it might also form isotropic gels mediated by counterions. Pf1 is 2 microns long, 6 nm in diameter, and in the absence of multivalent counterions remains isotropic at concentrations above 5 mg/ml. Divalent ions at concentrations well below those needed to form Pf1 bundles (Figure 3) induce the formation of elastic networks [12] with relatively low mechanical loss and Young's moduli (Figure 4) very close to those of vimentin networks stabilized by Mg^{2+}. Just as Mn^{2+} is a stronger bundling agent than Mg^{2+} (Figure 2), it is also a stronger gelation agent than Mg^{2+} for Pf1 (Figure 4) and the concentrations of divalent counterions needed for gelation are slightly affected but not eliminated in solutions of physiological ionic strength [12]. Since Pf1 has a relatively simple structure formed by a single coat protein with a short sequence of acidic amino acids at the virus surface [53], it seems unlikely that the virus has specific binding sites with different affinities for Mg^{2+} and Mn^{2+}, and therefore the possibility that gelation is caused by generic electrostatic effects rather than specific binding seems probable. The equivalence of the elastic moduli formed by vimentin crosslinked with Mg^{2+} and the gelled Pf1 virus network suggests that equivalent polyelectrolyte effects might also occur in other systems and perhaps are relevant in the cytoplasm.

Under the conditions in many biological fluids including the cytoplasm and sites of infection, the concentrations of filamentous polyelectrolytes are much higher (>10 mg/ml) than are generally studied or accessible in vitro. At these high concentrations of polymers and other solutes, multiple physical factors would affect filament network or bundle formation in addition to more specific protein-mediated effects usually assumed to dictate filament assembly in vivo. The long, extended shape of F-actin and other cytoskeletal polymers has bee shown to lead to formation of nematic phases at concentration > 2 mM even without counterion-mediated attractions or other bonds, and molecular crowding by other protein and macromolecules also contributes to filament reorganization. The interplay between excluded volume effects of counterion-mediated filament assembly has been studied for F-actin and other systems [21, 81, 82], and it is very likely that many important features will be revealed as studies in vitro approach more closely the conditions in vivo.

Estimate of divalent cation-mediated crosslink strength

The crosslinks formed by counterions in networks of anionic polyelectrolytes differ from covalent or noncovalent crosslinks formed by specific binding proteins in that they are easily disrupted by small forces, as occur when the networks are strained. As a result, networks of rigid or semiflexible polymers crosslinked only by counterions are not strain-stiffening, as they are when tightly crosslinked, but rather the networks soften at moderate strains, but rapidly reform when the stress generated by the deformation is relieved [12]. An estimate of the counterion crosslink strength has been obtained by comparing experiments of Pf1 virus with simulations [12], and these strengths are consistent with an analytic theory developed by Shklovskii et al [7, 83].

The fixed negative charges as well as the mobile counterions of valence Z on the Pf1 virus surface are strongly correlated and the theory developed by Shklovskii et al predicts that counterions condense to form a Wigner crystal, a 2D lattice that forms at low density to neutralize highly charged objects and minimize the potential energy on the virus surface due to this strong correlation[7, 84]. Assuming the Pf1 surface charge is neutralized by the counterions, the lattice spacing, ***r***, of the Wigner crystal is found by relating the surface area of the virus to the number of counterions, $\pi r^2 N_i = 2\pi RL$, where $\boldsymbol{N_i}$ is the number of counterions condensed on the viral surface, ***R*** is the radius of a Pf1 virus and ***L*** is the length of Pf1. For Pf1, ***R*** = 3 nm, ***L*** = 2000 nm. A Pf1 virus carries a total negative charge of 19,100e [54]. The number of divalent ions on a virus $\boldsymbol{N_i}$ is then 9550, and $\boldsymbol{r} \approx 1.12$ nm.

When two viruses come into contact with each other in an orthogonal configuration, at the spot where the viruses overlap the density of negative charges (from Pf1) is doubled, and the counterion density (from the Wigner crystal) is also doubled. In this region, the effective lattice spacing of the Wigner crystal is decreased and the free energy per ion is reduced as the counterions redistribute to have the same electrochemical potential [85]. This effect leads to a small contact region termed a “sticky patch” of cohesion between the two viruses. The sticky patch is a circular disk of radius $W = \sqrt{\gamma r R}$, where $\gamma = \sqrt{3}/2\pi \sim 0.3$. The size of the sticky region for two perpendicular Pf1 viruses given these parameters, $W = \sqrt{0.3(1.12\,\mathrm{nm})(3\,\mathrm{nm})}$ is about 1 nanometer and can be seen by plotting the contours of equidistant lines between two cylinders in Figure 5.

The free energy change in the sticky patch can be found by computing the chemical potential per counterion as the derivative of the correlation energy between counterions in the contact region,

$$E_{\mathrm{ion}} = -\alpha \frac{1.6 z^2 e^2}{4\pi\varepsilon\varepsilon_0 r}$$

The parameter α describes the packing of mobile ions in the sticky patch and depends on both the geometry of the contact region and the dielectric properties of the polyelectrolyte

filament. It is always less than 0.3 [83]. For divalent ions interacting with two Pf1 viruses in contact with each other, $E_{ion} \sim -5.5\times10^{-21}$ Joule = $-1.5\ k_B T$.

The total free energy change is determined by calculating ***n*** the number of counterions from each virus in the sticky region from the surface density of counterions as,

$$n=\pi W^2 \frac{N_i}{2\pi RL}=\frac{N_i \gamma r}{2L}.$$

Using the parameters of Pf1 virus $\boldsymbol{n} \approx 1$, i.e. each virus contributes one counterion to the sticky region, and therefore there are a total of 2 additional counterions in the 1 nm contact patch. Hence the total energy change of the system due to the counterion-mediated attraction per crosslink is

$$E=2E_{\mathrm{ion}}\sim -3\,k_{\mathrm{B}}T.$$

Assuming that a crosslink breaks when the virus separation is > 2nm, the corresponding estimate for breaking force is 6 pN, which is an upper limit based on α= 0.3 and other simplifying assumptions.

This attractive interaction can be strong enough to crosslink the viruses and form a network or gel. Comparison of experiments in which Pf1 gels such as those in Figure 4 were strained until the value of G′ abruptly decreased, presumably because of crosslink failure, with computer simulations to estimate the average force per crosslink at the breaking point, suggest a value of <0.4 pN as the critical breaking force, consistent with lower dielectric constant of the virus which would decrease α [12]. In contrast, actin crosslinking proteins such as filamin or alpha actinin have rupture forces on the order of 40 pN [86].

Quantitative estimates derived from theory therefore show that counterion-mediated crosslinking of isotropic suspensions of polyelectrolyte filaments can produce networks with measureable elastic moduli, but that such networks are fragile to strains that a more permanent crosslinker such as a protein can withstand. Such interactions might contribute to the rheology of the cytoskeleton but do not replicate the stronger effects of specific crosslinking agents.

Intracellular polyelectrolytes in extracellular fluids

Separating polyelectrolyte effects on cytoskeletal or nuclear filament crosslinking and bundle formation from the effects of the myriad proteins that bind to the filament sides in order to perform well-conserved and regulated functions is challenging. However, when polymers that have well-conserved intracellular functions are released into extracellular environments in which they have no biological function, the structures and interactions that occur in these settings are likely to result from generic physical-chemical effects rather than from specific biologically evolved binding events. For example, after trauma or necrosis of cells as occurs in chronic infections, nuclear and cytoskeletal filaments are released into the

extracellular space where highly charged anionic polymers are typically scarce. Extracellular fluids have proteins, small solutes, and ionic compositions that differ strongly from those of the cytoplasm, and when highly charged polyelectrolytes enter these fluids significant pathological effects can occur. For example, the airway fluid in lung, where F-actin and DNA accumulate in CF has cation concentrations of 64 mM Na^+, 2.4 mM K^+, 1.9 mM Mg^{2+}, and 1.2 mM Ca^{2+} [87]. In contrast, the cytoplasm has 12 mM Na^+, 139 mM K^+, 0.8 mM Mg^{2+}, and < 0.001 mM Ca^{2+} [88]. The much greater concentrations of divalent cations in airway fluid and blood plasma as well as the lower ionic strength of airway fluid would both tend to enhance the bundling of anionic polyelectrolytes such as DNA [89] and F-actin that are released mainly from dying cells, and there are mechanisms to clear these polymers from the bloodstream [90, 91]. In cases where this system is overwhelmed or when these polymers enter other extracellular compartments such as the lung airway fluid, both DNA and F-actin assemble into very large and stable structures (Figure 6). The aggregates formed by DNA and F-actin in extracellular fluids alter their viscosity or viscoelasticity and often inactivate polyvalent cationic antimicrobial agents such as those discussed in Figure 2. Among the many damaging effects of extracellular DNA and F-actin are promotion of biofilm growth [92, 93] and inactivation of antimicrobial defenses [65, 94, 95]. The effects of polyelectrolytes on biofilms might also be related to the finding that a filamentous virus similar to Pf1 is strongly upregulated in bacteria that start producing biofilms and might contribute directly to biofilm formation [96].

Figure 6 shows that very large bundles of DNA are found in both pus from a skin infection (B) and sputum from a cystic fibrosis (CF) patient (D). Actin aggregates are also found in CF sputum [97, 98] (Figure 6C). The fact that F-actin and DNA released from cells into the extracellular fluid assemble into large fibers that do not form intracellularly and with dimensions often larger than the cell suggests that they are reorganized into bundles by solutes in the extracellular fluid. A number of cationic proteins and peptides have been detected within such bundles. These include histones that are released with DNA from the nucleus, but also the cationic extracellular enzyme lysozyme, the antimicrobial peptide LL37 [94, 99], and cationic inflammatory mediators such as IL-8 [100]. The effects of the abundant cationic antibacterial enzyme lysozyme on polyelectrolytes have been especially well studied as a model for electrostatic interactions between proteins and oppositely charged filaments. In solutions containing 150 mM monovalent salt, F-actin is bundled by 4 μm lysozyme [99], DNA by 8 μM [68] and HA forms rodlike complexes with lysozyme when the two macroions are present at equal ionic concentrations [101].

The effect of polycations on anionic polyelectrolytes in extracellular fluids is not limited to the formation of large filament bundles that increase fluid viscosity. The sequestration of polycationic solutes into these bundles also inhibits their functions, potentially contributing to the failure of antimicrobial agents to function at sites of chronic infection. Both F-actin and DNA inhibit the ability of LL37, beta defensin, lysozyme, and other cationic antimicrobial agents to kill bacteria [65, 94, 95, 102], presumably because the anionic polyelectrolytes compete with the negatively charged bacteria for binding the cationic antimicrobials. This effect is not limited to native components of the innate immune system, but extends to antibiotic drugs such as tobramycin which is also polycationic. A X-ray scattering study of tobramycin bound within DNA bundles [103] reveals how this cationic

drug is sequestered within DNA bundles and therefore cannot access its target bacteria (Figure 6B).

The hypothesis that bacterial survival and biofilm formation is promoted by the interaction of cationic antimicrobial agents and the linear polyelectrolytes that accumulate at sites of infection has motivated efforts to exploit the principles of polyelectrolyte systems to design improved strategies that enable antibacterial function within chronic infection sites. Perhaps the first such strategy was to administer DNase1 in cystic fibrosis to depolymerize the large bundles of DNA present in sputum [104, 105]. The original aim was to reduce the abnormal high elastic moduli of CF sputum, but in addition to this effect, there is also a reduced incidence of infection [106]. Studies in vitro show that as the length of DNA in CF sputum is decreased by DNase, or when actin filaments are severed by the protein gelsolin, antimicrobial agents trapped in these bundles regain the ability to kill resident bacteria [65, 94]. The effects of DNase and gelsolin, which reduce the length of the polyelectrolytes but do not neutralize the charge on their subunits or fragments suggests that generic counterion condensation effects rather than specific binding of DNA or actin to antimicrobial agents leads to the functional effects of these polymers in sputum. Several other strategies based on polyelectrolyte effects have been tested to restore antibacterial function. In one, soluble multivalent co-ions such as the anionic oligomer polyaspartate have been shown to dissolve actin/DNA bundles and restore antibacterial activity in both CF sputum and mixtures of DNA and F-actin [65, 68, 93] (Figure 6C,D). The opposite approach, to add multivalent counterions such as polycationic amphiphiles with strong negative curvature preference can also displace trapped cationic antibiotics [103]. Finally, efforts to reduce the positive charge of antimicrobial agents or to distribute it over larger surface have also shown potential to retain antibacterial activity in fluids with high concentrations of F-actin and DNA [67, 107–110].

Conclusion

Linear polymers with large negative charge densities that display properties of strong polyelectrolytes are common in the nucleus and cytoskeleton of most cells, but are relatively scarce in the extracellular space. The interactions between polyelectrolytes and their counterions lead to a large number of ordered phases that can be controlled in vitro by varying polyelectrolyte length, stiffness, and concentration and by the concentration and valence of counterions and co-ions in solution. The biological relevance of such effects are becoming increasingly evident studies of intracellular polymers released into extracellular environments and might also contribute to the structural, mechanical, and biochemical properties of these polymers in vivo.

Acknowledgments

This work was supported by National Science Foundation grant DMR11-20901 and National Institute of Health grants DK083592 and T32-HL07954.

References

1. Manning GS. Journal of Physical Chemistry B. 2007; 111:8554–8559.
2. Manning GS. Biophys Chem. 1978; 9:65–70. [PubMed: 753405]

3. Sayar M, Holm C. Phys Rev E Stat Nonlin Soft Matter Phys. 2010; 82:031901. [PubMed: 21230102]
4. Fischer S, Naji A, Netz RR. Phys Rev Lett. 2008; 101:176103. [PubMed: 18999768]
5. Manning GS. Q Rev Biophys. 1978; 11:179–246. [PubMed: 353876]
6. Wilson RW, Rau DC, Bloomfield VA. Biophys J. 1980; 30:317–325. [PubMed: 7260278]
7. Shklovskii BI. Phys Rev Lett. 1999; 82:3268–3271.
8. Wong GC, Pollack L. Annu Rev Phys Chem. 2010; 61:171–189. [PubMed: 20055668]
9. Huber F, Strehle D, Kas J. Soft Matter. 2012; 8:931–936.
10. Deshpande S, Pfohl T. Biomicrofluidics. 2012:6.
11. Kwon HJ, Kakugo A, Ura T, Okajima T, Tanaka Y, Furukawa H, Osada Y, Gong JP. Langmuir. 2007; 23:6257–6262. [PubMed: 17461601]
12. Huisman EM, Wen Q, Wang YH, Cruz K, Kitenbergs G, Erglis K, Zeltins A, Cebers A, Janmey PA. Soft Matter. 2011; 7:7257–7261. [PubMed: 22267963]
13. Wong GC, Lin A, Tang JX, Li Y, Janmey PA, Safinya CR. Phys Rev Lett. 2003; 91:018103. [PubMed: 12906579]
14. Muhlrad A, Grintsevich EE, Reisler E. Biophys Chem. 2011; 155:45–51. [PubMed: 21411219]
15. Needleman DJ, Ojeda-Lopez MA, Raviv U, Miller HP, Wilson L, Safinya CR. Proceedings of the National Academy of Sciences of the United States of America. 2004; 101:16099–16103. [PubMed: 15534220]
16. Sowa GZ, Cannell DS, Liu AJ, Reisler E. Journal of Physical Chemistry B. 2006; 110:22279–22284.
17. Zribi OV, Kyung H, Golestanian R, Liverpool TB, Wong GC. Phys Rev E Stat Nonlin Soft Matter Phys. 2006; 73:031911. [PubMed: 16605562]
18. Eickbush TH, Moudrianakis EN. Cell. 1978; 13:295–306. [PubMed: 203402]
19. Kaur H, Kumar S, Singh K, Bharadwaj LM. Int J Biol Macromol. 2011; 48:793–797. [PubMed: 21397632]
20. Tang JX, Kas JA, Shah JV, Janmey PA. Eur Biophys J. 2001; 30:477–484. [PubMed: 11820391]
21. Cebers A, Dogic Z, Janmey PA. Phys Rev Lett. 2006; 96:247801. [PubMed: 16907280]
22. Evans HM, Ahmad A, Ewert K, Pfohl T, Martin-Herranz A, Bruinsma RF, Safinya CR. Phys Rev Lett. 2003; 91:075501. [PubMed: 12935030]
23. Koltover I, Wagner K, Safinya CR. Proc Natl Acad Sci U S A. 2000; 97:14046–14051. [PubMed: 11121015]
24. Lee KC, Borukhov I, Gelbart WM, Liu AJ, Stevens MJ. Phys Rev Lett. 2004; 93:128101. [PubMed: 15447308]
25. Ermoshkin AV, Olvera de la Cruz M. Phys Rev Lett. 2003; 90:125504. [PubMed: 12688884]
26. Borukhov I, Bruinsma RF. Phys Rev Lett. 2001; 87:158101. [PubMed: 11580726]
27. Korolev N, Allahverdi A, Lyubartsev AP, Nordenskiold L. Soft Matter. 2012; 8:9322–9333.
28. Janmey, P.; MacKintosh, FC. Polymers in biology and medicine. Langer, RS.; Tirrell, DA., editors. Vol. 9. Elsevier; Amsterdam: 2012. p. 183-200.
29. Wen Q, Janmey PA. Current Opinion in Solid State & Materials Science. 2011; 15:177–182. [PubMed: 22081758]
30. Tang JX, Wong SE, Tran PT, Janmey PA. Berichte Der Bunsen-Gesellschaft-Physical Chemistry Chemical Physics. 1996; 100:796–806.
31. Khurana S. J Membr Biol. 2000; 178:73–87. [PubMed: 11083897]
32. dos Remedios CG, Chhabra D, Kekic M, Dedova IV, Tsubakihara M, Berry DA, Nosworthy NJ. Physiol Rev. 2003; 83:433–473. [PubMed: 12663865]
33. Giometti CS, Anderson NL. J Biol Chem. 1984; 259:14113–14120. [PubMed: 6501290]
34. Cohen C, Longley W. Science. 1966; 152:794–796. [PubMed: 17797461]
35. Stewart M, McLachlan AD. Nature. 1975; 257:331–333. [PubMed: 1161036]
36. Lorenz M, Poole KJ, Popp D, Rosenbaum G, Holmes KC. J Mol Biol. 1995; 246:108–119. [PubMed: 7853391]

37. Metalnikova NA, Tsaturyan AK. Biophys J. 2013; 105:941–950. [PubMed: 23972846]
38. Cunningham CC, Leclerc N, Flanagan LA, Lu M, Janmey PA, Kosik KS. J Cell Biol. 1997; 136:845–857. [PubMed: 9049250]
39. Griffith LM, Pollard TD. J Cell Biol. 1978; 78:958–965. [PubMed: 568144]
40. Petrucci TC, Morrow JS. J Cell Biol. 1987; 105:1355–1363. [PubMed: 3115996]
41. Hurley SL, Brown DL, Cheetham JJ. Biochem Biophys Res Commun. 2004; 317:16–23. [PubMed: 15047142]
42. Tsvetkov AS, Samsonov A, Akhmanova A, Galjart N, Popov SV. Cell Motil Cytoskeleton. 2007; 64:519–530. [PubMed: 17342765]
43. Fujii T, Takagi H, Arimoto M, Ootani H, Ueeda T. J Biochem. 2000; 127:457–465. [PubMed: 10731718]
44. Sun D, Leung CL, Liem RK. J Cell Sci. 2001; 114:161–172. [PubMed: 11112700]
45. Svitkina TM, Verkhovsky AB, Borisy GG. J Cell Biol. 1996; 135:991–1007. [PubMed: 8922382]
46. Sevcik J, Urbanikova L, Kost'an J, Janda L, Wiche G. Eur J Biochem. 2004; 271:1873–1884. [PubMed: 15128297]
47. Forlemu NY, Njabon EN, Carlson KL, Schmidt ES, Waingeh VF, Thomasson KA. Proteins. 2011; 79:2813–2827. [PubMed: 21905108]
48. Vertessy BG, Orosz F, Kovacs J, Ovadi J. J Biol Chem. 1997; 272:25542–25546. [PubMed: 9325270]
49. Tang JX, Janmey PA. J Biol Chem. 1996; 271:8556–8563. [PubMed: 8621482]
50. Bloomfield VA. Biopolymers. 1997; 44:269–282. [PubMed: 9591479]
51. Podrazky V, Stokrova S, Fric I. Connect Tissue Res. 1975; 4:51–54. [PubMed: 3386]
52. Oosawa, F. Polyelectrolytes. Marcel Dekker, Inc; 1971.
53. Crowther RA. Nature. 1980; 286:440–441. [PubMed: 7402326]
54. Zimmermann K, Hagedorn H, Heuck CC, Hinrichsen M, Ludwig H. J Biol Chem. 1986; 261:1653–1655. [PubMed: 3944103]
55. Haxaire K, Braccini I, Milas M, Rinaudo M, Perez S. Glycobiology. 2000; 10:587–594. [PubMed: 10814700]
56. Smith TA, Hempstead PD, Palliser CC, Parry DA. Proteins. 2003; 50:207–212. [PubMed: 12486714]
57. Meng JJ, Khan S, Ip W. J Biol Chem. 1994; 269:18679–18685. [PubMed: 8034617]
58. Aranda-Espinoza H, Carl P, Leterrier JF, Janmey P, Discher DE. FEBS Lett. 2002; 531:397–401. [PubMed: 12435582]
59. Deek J, Chung PJ, Kayser J, Bausch AR, Safinya CR. Nat Commun. 2013; 4:2224. [PubMed: 23892390]
60. Gou JP, Gotow T, Janmey PA, Leterrier JF. Med Biol Eng Comput. 1998; 36:371–387. [PubMed: 9747580]
61. Beck R, Deek J, Choi MC, Ikawa T, Watanabe O, Frey E, Pincus P, Safinya CR. Langmuir. 2010; 26:18595–18599. [PubMed: 21082794]
62. Leterrier JF, Kas J, Hartwig J, Vegners R, Janmey PA. J Biol Chem. 1996; 271:15687–15694. [PubMed: 8663092]
63. Lin YC, Broedersz CP, Rowat AC, Wedig T, Herrmann H, Mackintosh FC, Weitz DA. J Mol Biol. 2010; 399:637–644. [PubMed: 20447406]
64. Ma C, Bloomfield VA. Biophys J. 1994; 67:1678–1681. [PubMed: 7819499]
65. Bucki R, Byfield FJ, Janmey PA. Eur Respir J. 2007; 29:624–632. [PubMed: 17215317]
66. Bucki R, Cruz K, Janmey P. Biophysical J. 2013; 104:256a.
67. Bucki R, Sostarecz AG, Byfield FJ, Savage PB, Janmey PA. J Antimicrob Chemother. 2007; 60:535–545. [PubMed: 17584802]
68. Tang JX, Wen Q, Bennett A, Kim B, Sheils CA, Bucki R, Janmey PA. Am J Physiol Lung Cell Mol Physiol. 2005; 289:L599–605. [PubMed: 15964901]
69. Koltover I, Salditt T, Safinya CR. Biophys J. 1999; 77:915–924. [PubMed: 10423436]

70. Bilalov A, Olsson U, Lindman B. Soft Matter. 2011; 7:730–742.
71. Wong GC, Tang JX, Lin A, Li Y, Janmey PA, Safinya CR. Science. 2000; 288:2035–2039. [PubMed: 10856215]
72. Safinya CR, Raviv U, Needleman DJ, Zidovska A, Choi MC, Ojeda-Lopez MA, Ewert KK, Li Y, Miller HP, Quispe J, Carragher B, Potter CS, Kim MW, Feinstein SC, Wilson L. Adv Mater. 2011; 23:2260–2270. [PubMed: 21506171]
73. Angelini TE, Liang H, Wriggers W, Wong GC. Eur Phys J E Soft Matter. 2005; 16:389–400. [PubMed: 19177656]
74. Beck R, Deek J, Safinya CR. Biochem Soc Trans. 2012; 40:1027–1031. [PubMed: 22988859]
75. Gartzke J, Lange K. Am J Physiol Cell Physiol. 2002; 283:C1333–1346. [PubMed: 12372794]
76. Lange K. J Theor Biol. 2000; 206:561–584. [PubMed: 11013115]
77. Gardel ML, Shin JH, MacKintosh FC, Mahadevan L, Matsudaira P, Weitz DA. Science. 2004; 304:1301–1305. [PubMed: 15166374]
78. Leterrier JF, Eyer J. Biochem J. 1987; 245:93–101. [PubMed: 3663160]
79. Yao NY, Broedersz CP, Lin YC, Kasza KE, Mackintosh FC, Weitz DA. Biophys J. 2010; 98:2147–2153. [PubMed: 20483322]
80. Kang HR, Bradley MJ, McCullough BR, Pierre A, Grintsevich EE, Reisler E, De La Cruz EM. Proceedings of the National Academy of Sciences of the United States of America. 2012; 109:16923–16927. [PubMed: 23027950]
81. Dogic Z, Fraden S. Current Opinion in Colloid & Interface Science. 2006; 11:47–55.
82. Tang JX, Ito T, Tao T, Traub P, Janmey PA. Biochemistry. 1997; 36:12600–12607. [PubMed: 9376366]
83. Zhang R, Shklovskii BI. Physical Review E. 2004; 69:021909.
84. Grosberg AY, Nguyen TT, Shklovskii BI. Reviews of Modern Physics. 2002; 74:329–345.
85. Rouzina I, Bloomfield VA. Journal of Physical Chemistry. 1996; 100:9977–9989.
86. Ferrer JM, Lee H, Chen J, Pelz B, Nakamura F, Kamm RD, Lang MJ. Proc Natl Acad Sci U S A. 2008; 105:9221–9226. [PubMed: 18591676]
87. Baconnais S, Tirouvanziam R, Zahm JM, de Bentzmann S, Peault B, Balossier G, Puchelle E. Am J Respir Cell Mol Biol. 1999; 20:605–611. [PubMed: 10100991]
88. Lang F. J Am Coll Nutr. 2007; 26:613S–623S. [PubMed: 17921474]
89. Pisetsky DS, Fairhurst AM. Autoimmunity. 2007; 40:281–284. [PubMed: 17516210]
90. Janmey PA, Lind SE. Blood. 1987; 70:524–530. [PubMed: 3038216]
91. Lee WM, Galbraith RM. N Engl J Med. 1992; 326:1335–1341. [PubMed: 1314333]
92. Walker TS, Tomlin KL, Worthen GS, Poch KR, Lieber JG, Saavedra MT, Fessler MB, Malcolm KC, Vasil ML, Nick JA. Infect Immun. 2005; 73:3693–3701. [PubMed: 15908399]
93. Parks QM, Young RL, Poch KR, Malcolm KC, Vasil ML, Nick JA. J Med Microbiol. 2009; 58:492–502. [PubMed: 19273646]
94. Weiner DJ, Bucki R, Janmey PA. Am J Respir Cell Mol Biol. 2003; 28:738–745. [PubMed: 12600826]
95. Jones EA, McGillivary G, Bakaletz LO. Journal of Innate Immunity. 2013; 5:24–38. [PubMed: 22922323]
96. Webb JS, Lau M, Kjelleberg S. J Bacteriol. 2004; 186:8066–8073. [PubMed: 15547279]
97. Sheils CA, Kas J, Travassos W, Allen PG, Janmey PA, Wohl ME, Stossel TP. Am J Pathol. 1996; 148:919–927. [PubMed: 8774146]
98. Vasconcellos CA, Allen PG, Wohl ME, Drazen JM, Janmey PA, Stossel TP. Science. 1994; 263:969–971. [PubMed: 8310295]
99. Sol A, Blotnick E, Bachrach G, Muhlrad A. Plos One. 2012:7.
100. Perks B, Shute JK. Am J Respir Crit Care Med. 2000; 162:1767–1772. [PubMed: 11069810]
101. Morfin I, Buhler E, Cousin F, Grillo I, Boue F. Biomacromolecules. 2011; 12:859–870. [PubMed: 21381699]
102. Lewenza S. Front Microbiol. 2013; 4:21. [PubMed: 23419933]

103. Purdy Drew KR, Sanders LK, Culumber ZW, Zribi O, Wong GC. Journal of the American Chemical Society. 2009; 131:486–493. [PubMed: 19072156]
104. Shak S, Capon DJ, Hellmiss R, Marsters SA, Baker CL. Proc Natl Acad Sci U S A. 1990; 87:9188–9192. [PubMed: 2251263]
105. Lieberman J. JAMA. 1968; 205:312–313. [PubMed: 5694947]
106. McPhail GL, Acton JD, Fenchel MC, Amin RS, Seid M. J Pediatr. 2008; 153:752–757. [PubMed: 18760423]
107. Scanlon TC, Teneback CC, Gill A, Bement JL, Weiner JA, Lamppa JW, Leclair LW, Griswold KE. Acs Chemical Biology. 2010; 5:809–818. [PubMed: 20604527]
108. Sanders LK, Xian W, Guaqueta C, Strohman MJ, Vrasich CR, Luijten E, Wong GC. Proc Natl Acad Sci U S A. 2007; 104:15994–15999. [PubMed: 17911256]
109. Bucki R, Leszczynska K, Byfield FJ, Fein DE, Won E, Cruz K, Namiot A, Kulakowska A, Namiot Z, Savage PB, Diamond SL, Janmey PA. Antimicrob Agents Chemother. 2010; 54:2525–2533. [PubMed: 20308375]
110. Fein DE, Bucki R, Byfield F, Leszczynska K, Janmey PA, Diamond SL. Mol Pharmacol. 2010; 78:402–410. [PubMed: 20573781]
111. Dolinsky TJ, Czodrowski P, Li H, Nielsen JE, Jensen JH, Klebe G, Baker NA. Nucleic Acids Res. 2007; 35:W522–525. [PubMed: 17488841]
112. Dolinsky TJ, Nielsen JE, McCammon JA, Baker NA. Nucleic Acids Res. 2004; 32:W665–667. [PubMed: 15215472]
113. Baker NA, Sept D, Joseph S, Holst MJ, McCammon JA. Proc Natl Acad Sci U S A. 2001; 98:10037–10041. [PubMed: 11517324]
114. Dammann C, Noding B, Koster S. Biomicrofluidics. 2012:6.
115. Tang JX, Janmey PA, Lyubartsev A, Nordenskiold L. Biophys J. 2002; 83:566–581. [PubMed: 12080143]
116. Osland A, Kleppe K. Nucleic Acids Res. 1977; 4:685–695. [PubMed: 17099]
117. Pelta J, Livolant F, Sikorav JL. J Biol Chem. 1996; 271:5656–5662. [PubMed: 8621429]
118. Wang, Y-H. PhD PhD. University of Pennsylvania; 2013.

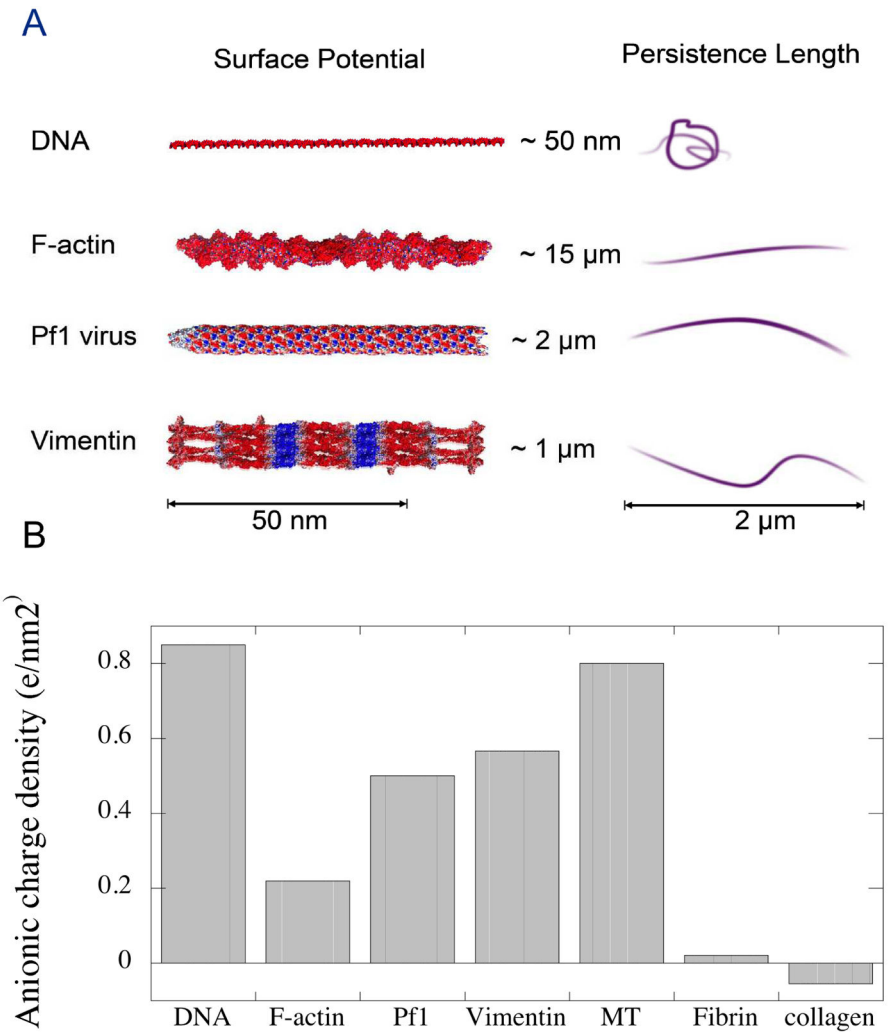

Figure 1.

Left: Electrostatic potential plotted on an inflated van der Waals surface of the polyelectrolytes. The electrostatic potential maps were computed using the PDB2PQR package [111, 112] to assign charges to the atoms and the APBS package [113] to solve the Poisson-Boltzmann equation numerically on a grid. Red is negative and blue is positive; colors are not normalized between molecules. Sketches on the right show persistence lengths for long polymers of the corresponding polyelectrolytes on the left and can be taken to represent the configuration of a 2 um polymer of the polyelectrolytes. Right: average surface charge density of various protein and polysaccharide polymers estimated from the net charge of the protein or polysaccharide, the mass/length ratios estimates as previously summarized [28, 29] and effective diameters of 2, 3, 6, 6, 10, 10, 25 for DNA, collagen microfibril, Pf1, F-actin, fibrin protofibril, vimentin, and microtubules, respectively.

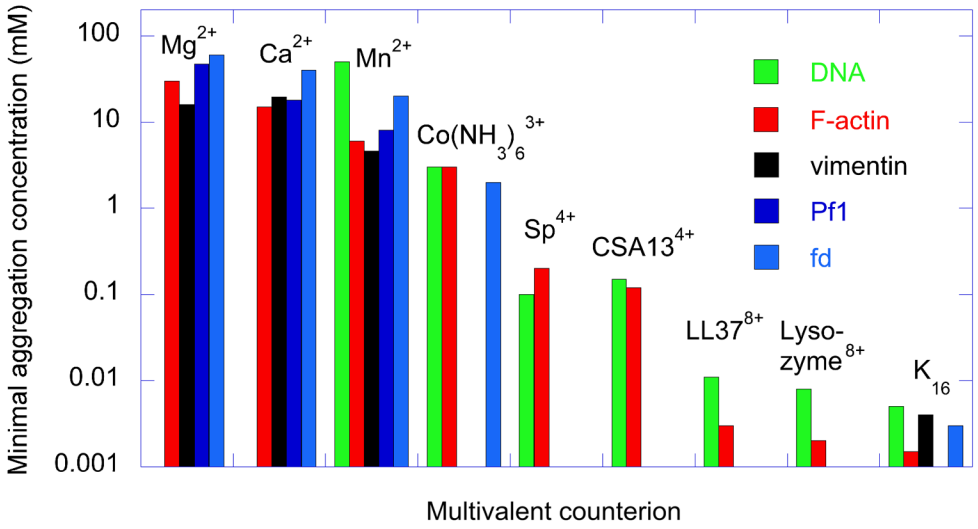

Figure 2.

Critical concentrations of various counterions require to induce bundle formation by diverse bio-polyelectrolytes as detected by abrupt increases in light scattering intensity or hydrodynamic diameter. Data for F-actin taken from [30, 49], for CSA13 from [67], LL37 from [94, 99], vimentin from [82, 114], Pf1 from [12], fd from [115], Lys18 from [30], F-actin/spermine from [14], DNA and spermine from [116], DNA and cobalt hexamine from [117].

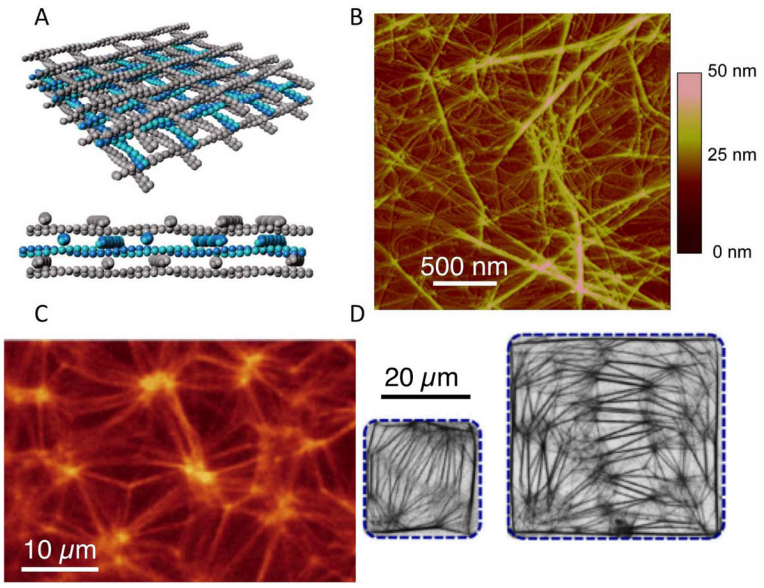

Figure 3.

A. Schematic of crosslinked raft phase of polyelectrolyte filaments and divalent cations from [13] reproduced by permission of the American Physical Society. B. Network phase of Pf1 virus with 5 mM Mn^{2+} from [118]. C,D Networks of actin bundles formed by increasing Mg2+ (~50 mM) as well as F-actin concentrations by evaporation of water from mixtures using in confined volumes without generating mixing flows. Adapted from refs [9] (C) reproduced by permission of The Royal Society of Chemistry (RSC) on behalf of Soft Matter and the RSC and [10] (D) by permission of AIP Publishing.

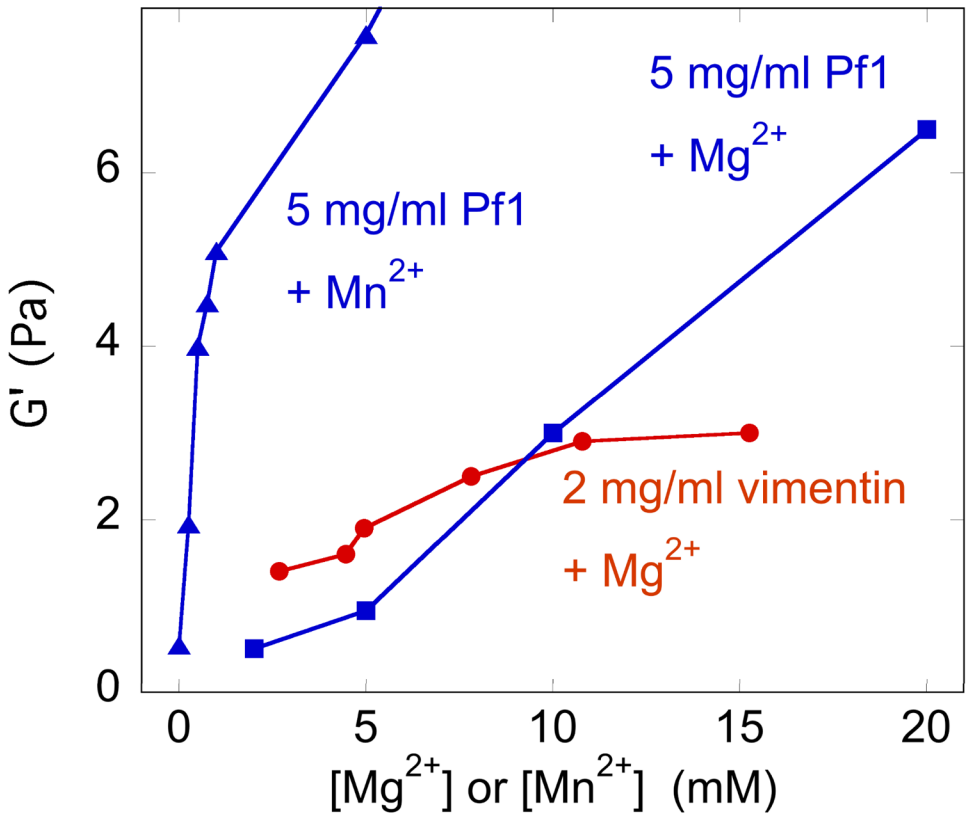

Figure 4.

Elastic network formation by vimentin and Pf virus induced by Mn^{2+} or Mg^{2+} at concentrations below the bundling transition. Vimentin data obtained from [63]; Pf1 data from [12].

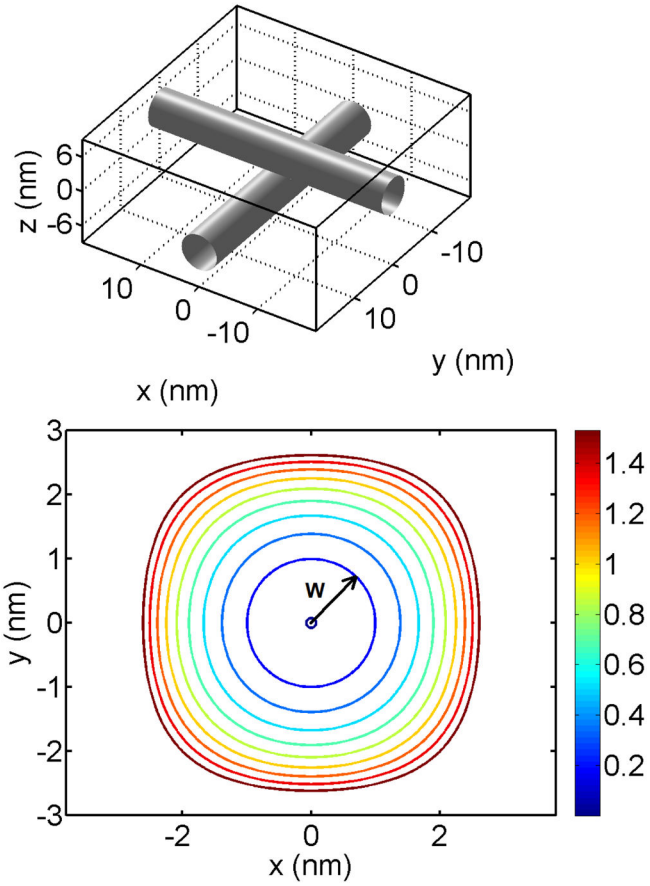

Figure 5.

Perpendicular cylinders and equi-distance plots between the surface of cylinders. Top: geometry and dimensions of two Pf1 viruses touching at right angles. Bottom: contour plots of the distance between virus surfaces (color map in nm) at different radial distances from the point of contact.

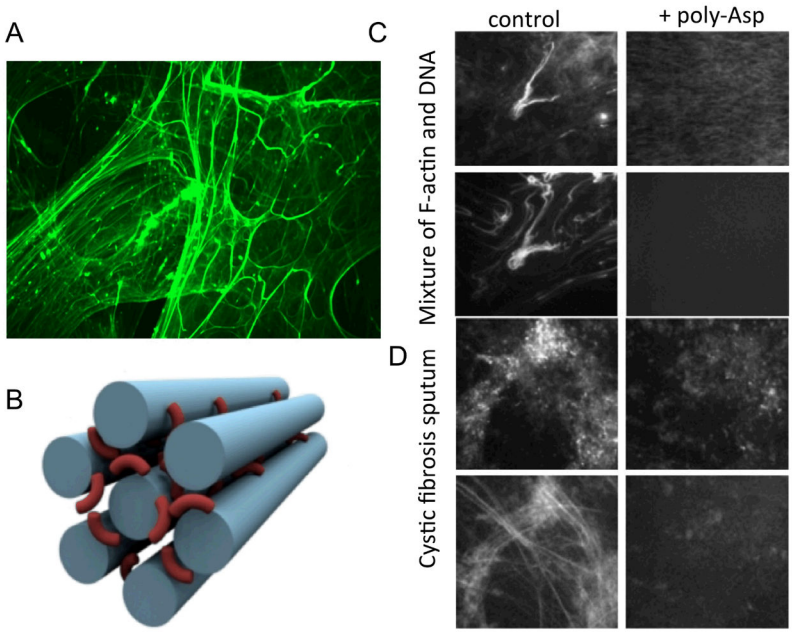

Figure 6.

DNA bundles in pus [66] (A). Structure of DNA bundles stabilized by the cationic antimicrobial drug tobramycin reprinted with permission from [103] copyright 2009 American Chemical Society. (B). Mixture of purified F-actin and DNA bundled by the antimicrobial peptide LL37 (C) or endogenous in CF sputum (D) before and after dissolution by poly-Asp [65]. Adapted from [103] (B) and [68] (C,D) reprinted with permission from the American Physiological Society.